International Journal of Fluid Power 11 (2010) No. 1 pp. 33-45

A NUMERICAL APPROACH FOR THE EVALUATION OF THE EFFECTS OF AIR RELEASE AND VAPOUR CAVITATION ON EFFECTIVE FLOW RATE OF AXIAL PISTON MACHINES

Andrea Vacca[1], Richard Klop[2] and Monika Ivantysynova[2]

[1]*Industrial Engineering Department - University of Parma, Italy*
[2]*MAHA Fluid Power Lab., Purdue University, West Lafayette (IN), USA*
andrea.vacca@unipr.it; rklop@purdue.edu; mivantys@purdue.edu

Abstract

This work illustrates a numerical methodology for the description of effective flow rate of axial piston pumps and motors. The presented mathematical model is similar to classical lumped parameter approaches that are commonly used to simulate hydraulic units; however, this work uniquely utilises a mathematical formulation for compressible flows based on an original description of fluid density. Assuming the behaviour of typical mineral oil, the model can evaluate fluid density for all possible values of pressure while considering the occurrence of gas cavitation (due to the release of air normally dissolved into liquid) below saturation pressure, and of vapour cavitation (due to liquid change of phase) below vapour pressure.

The developed simulation model allows a description of several characteristics of the machine (i.e. instantaneous cylinder pressure and density, delivery and inlet flow rates, etc.) in its whole field of operation taking into account conditions of insufficient flow due to cavitation at the low pressure port.

Tests were carried out on a swash plate type axial piston pump for open circuit applications to verify potentials of the developed numerical model. Experiments were conducted to test the pump under typical operating conditions as well as situations critical from the point of view of cavitation (high shaft speed, low values of inlet pressure), thus permitting the comparison between the prediction given by the developed model and experimental results over a wide range of data.

Results highlight how fluid density changes can be used to characterize effective flow rate but also to justify, in particular operating conditions, the utilization of the approach for compressible flows. Results show that the developed model uniquely allows the calculation of effective flow rate through the pump at fair and extreme conditions, thus permitting the ability to predict limitations of the machine. Furthermore, the realistic prediction of pressures throughout the machine in these conditions leads the accurate predictions of pressure forces and of flow through the lubricating gaps that may be critical in other models.

Keywords: numerical models, cavitation, axial piston pumps, fluid properties

1 Introduction

Nowadays, axial piston pumps and motors are often the preferred choice of energy conversion units in many fluid power applications. Reasons of success of these types of units lie in their simple structure, high reliability, elevated efficiencies and high operating pressures. The number of applications of axial piston machines is expected to increase. Axial piston machines can be designed as variable displacement machines which make them suitable for several new system applications like displacement control actuation and new continuously variable transmissions and hybrid power trains. Thus, the market share for variable displacement machines has continuously increased over the last 30 years and the demand towards energy savings will strengthen this trend.

Significant research on axial piston machines has appeared in literature within the last forty years. Most published works have been concerned with aspects related to control of variable displacement units and operating efficiency. More recently, many researchers have focused their attention on topics related to noise

This manuscript was received on 18 March 2009 and was accepted after revision for publication on 18 November 2009

emissions, in particular flow ripple and oscillating forces exerted on pump parts.

A significant portion of the mentioned research takes advantage of simple predictions of effective flow rate which include lumped parameter models based on continuity, state equation for liquids, and the orifice equation for incompressible turbulent flow. Some examples include Edge et al. (1989), Palmberg (1989), and Manring (2000) which utilize this type of simplified approach to perform studies concerning the analysis and the reduction of delivery pressure ripple of axial piston pumps. In Schoenau et al. (1990) and Kim et al., (1987) similar models were used inside wider models for the analysis of displacement control systems; while in Wieczorek and Ivantysynova (2002) and Ivantysynova et al. (2002) the same approach is used as a part of the in-house developed code CASPAR to investigate swash plate moments and flows through lubricating gaps in swash plate type axial piston machines. In Seeniraj and Ivantysynova (2008), a similar model was proposed to optimize valve plate designs for reduction of both flow ripple and oscillating forces on the swash plate. In Klop and Ivantysynova (2008), this type of model was extended to simulate a basic hydrostatic transmission by use of a suitable line model.

All mentioned works highlight the advantages given by adopting simple and fast approaches for the calculation of effective flow rate for analysis of various aspects related to design or control. However, there are cases where such simplified approaches can provide rough or incorrect estimations. These incorrect evaluations affect all calculation based on the estimated pressures or flow rates (like the forces acting on moving components of the pump, the flows into lubricating gaps, etc.). Obviously, this occurs when the limiting hypotheses made on the mathematical model are unsatisfied. In particular, a frequent assumption made in the mentioned models is the state equation for liquids used to evaluate fluid density, neglecting the influence of gas or vapour cavitation. Cavitation phenomena take place below saturation pressure[1]; the release of air normally dissolved into the fluid (gas cavitation) occurs in the form of bubbles for $p < p_{SAT}$ and vapour cavitation occurs for $p < p_{VAPH}$. Cavitation has erratic and local features and is an undesired phenomenon for hydraulic components; damages to mechanical parts can be caused from the formation of bubbles that collapse. Moreover, usually in case of positive displacement machines for open system circuits, cavitation can occur at the LP port, limiting the discharge flow rate of a pump.

Past attempts to model cavitating flow numerically can be roughly divided in two classes: interface tracking and continuous methods. Interface tracking is a technique for two-phase flows where each phase is treated separately. There are typically separate equations for conservation of mass and momentum of each phase, which more than doubles the cost of modelling the flow. Furthermore, a scheme for reconstructing the interface of the sub-cell level is required. For this purpose, there are several possibilities, as described in Hyman (1984). In continuous methods a distinct interface is not present and the two phases (gas and liquid) are considered to be the same fluid. Fluid properties, such as density, reflect the liquid and vapour contents. The continuum method is a convenient way of modelling the flow numerically, because it doesn't imply more equations than a single phase flow. The difficult part of developing such models is deriving meaningful and stable equations for the evaluation of fluid pressure and density. Significant examples of continuum methods are described in Delannoy et al. (1990), Schmidt et al. (1999) and Singhal et al. (2002) where a barotropic equation of state in which density is a function of pressure is used to simulate 2D cavitating flows. The proposed work considers a continuum method for the evaluation of fluid properties simpler than the mentioned one, being not based on the evaluation of bubbles' radius. The main objective of the proposed work is developing a numerical model for the evaluation of flow from the inlet port into the displacement chamber, and flow from the displacement chamber to the outlet port; the model considers main effects due to cavitation, and quantifying the amount of cavitation without providing detailed features about bubble formation, growth and collapse. The proposed model is an alternative to standard lumped parameter models commonly used to simulate axial piston machines; the model offers a wider range of applicability while obtaining the same features of simplicity and simulation swiftness.

In fluid power literature, it is possible to find few works concerning simplified models for the evaluation of effects due to cavitation on flow. As reported in Lamb (1987), a simple parameter, the cavitation number, can be used to quantify the amount of cavitation for flow across an orifice. Few models, like the one proposed in Schmidt et al. (1997), utilize this parameter to correct the discharge coefficient used in standard turbulent orifice equations. In LMS IMAGINE SA (2007), a simple model for the calculation of fluid density as a function of pressure suitable for lumped parameters models is described, and the same model is successfully applied for simulation of hydraulic systems in the commercial software AMESim®. Similarly, in Casoli et al. (2006), different and simple approaches for the calculation of fluid properties are presented and compared on the basis of results achieved using a simple fluid dynamic model of a hydraulic component. In particular, one of the approaches described in this latter work has been considered in the development of the proposed model, but rewriting it in an enhanced form.

One of the crucial points concerning lumped parameter models typically used in fluid power that consider a complex calculation of fluid properties is performing a consistent integration between the model for fluid properties and the equations used to solve for various flow rates. To achieve desired simplicity and simulation swiftness, the majority of the mentioned studies adopt approaches for incompressible flow, adding a correction of some equations in order to account for variable fluid density (with average values of density or defining correction coefficients). However, this can imply a rough prediction of flow in case of

1 For fluid power systems tank pressure, usually atmospheric pressure, can be assumed to be saturation pressure.

relevant incipient cavitation.

The proposed approach in this paper reassesses the standard lumped parameter models commonly used for the simulation of positive displacement machines by proposing a formulation valid for compressible flows, where fluid density is calculated considering a continuum also in case of cavitation.

To accomplish this result, the model implemented in the "CASPAR Pressure Module" software (Wieczorek et al., 2002) has been taken as an initial reference. In this paper, a novel set of equations describing fluid properties and features of flow has been developed and implemented in a new version of "CASPAR".

To verify predictions given by the new model, simulation results have been compared with experimental data. For this purpose, an open circuit swash plate type axial piston pump was tested up to conditions of incipient cavitation at the suction port.

The comparison between experimental data and simulation results is discussed and used to clarify how the model simulates the onset of cavitation for the considered machine. The discussion about simulation results also involves the range of validity of the standard approach based on the simple equations for liquids and for incompressible flows. In particular, results identify zones where the standard approach represents a good approximation of reality and the remaining zones where the effects of cavitation are more relevant and need to be described by compressible flow models. Results also show an accurate prediction of effective flow rate at extreme conditions which reveal limitations of the machine.

2 Modelling Fluid Properties

This section aims to define a reliable model for the calculation of fluid density over a wide range of pressures suitable for lumped parameter approaches for hydraulic components. As a consequence, the model must be characterized by a simple definition of the input parameters required for the description of fluid also in case of mineral oils (typically given by mixtures of components of different chemical nature).

The approach for the calculation of fluid properties considered in this study belongs to continuous methods. This permits modelling flow from the ports to and from the displacement chamber with equations typical for mono-phase flows. In particular, fluid density and its derivative are the main properties of fluid that characterize flow. For the calculation of these quantities the pressure field has been subdivided into four regions or zones (Fig. 1). Values for p_{SAT}, p_{VAPH}, p_{VAPL} are defined by the user as model's parameters. In this way, the model can take into account effects due to gas and vapour cavitation in a simple manner[2].

2 Vapour cavitation (described by regions 3 and 4 of Fig. 3) is an extreme condition for flow through common hydraulic components. However, it has been considered for the sake of generality of the proposed model and in order to formulate a numerical code also suitable for design purposes (during the design process it is convenient to use a code able to estimate also bad designs that can lead to vapour cavitation).

The approach for the calculation of fluid properties is comparable with the methodology described in IMAGINE SA (2007) and with one of the approaches presented in Casoli et al. (2006). In particular, with respect to Casoli's work, several improvements have been made in the formulation presented in this paper:

- possibility to use available experimental data for fluid density and bulk modulus as a function of pressure;
- calculation of effects due to fluid temperature (flow through the pump is not isothermal);
- consideration of different ranges of pressure that govern air release.

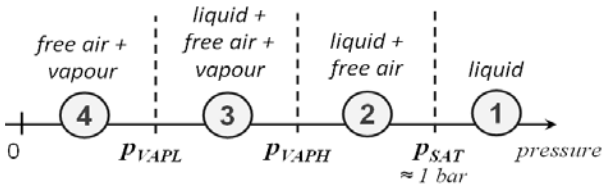

Fig. 1: *Four different zones considered for the calculation of fluid properties*

For each region, equations used for the calculation of fluid density are described:

2.1 Zone 1: Liquid

For $p > p_{SAT}$ the model is simply based on the state equation for liquids, where fluid density and bulk modulus are obtained by means of interpolations between values provided by the oil supplier (constant values can be used in case of lack of experimental data). For example in Fig. 2, data pertaining to the density of oil used during the experimental tests (see Section 5) are reported.

As concerns the value of parameter p_{SAT}, in this work it has been assumed p_{SAT} = 1.013 bar, assuming the equilibrium between liquid and air in a tank open to the atmosphere.

Similarly to classical lumped parameter models for hydraulic components, in this zone ($p > p_{SAT}$) the model assumes the incondensable gas (air) completely dissolved into liquid.

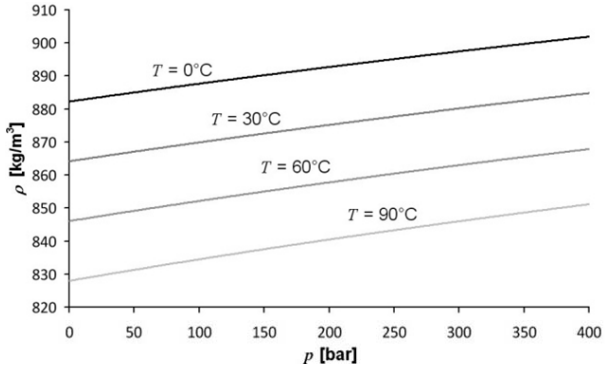

Fig. 2: *Density of HLP 32 mineral oil (gauge pressure)*

The value of the density derivative is therefore given by Eq. 1:

$$\left(\frac{\partial p}{\partial \rho}\right)_T\Bigg|_{p^*,T^*} = \frac{K(p^*,T^*)}{\rho(p^*,T^*)} \tag{1}$$

The model assumes that in this region experimental data include the mass effect of air dissolved into oil.

2.2 Zone 2: Liquid + Free Air

Below saturation pressure, the model calculates the amount of air dissolved into liquid as a function of fluid pressure with a relationship that approximates Dalton-Henry's law. In order to obtain a continuous derivative function also at boundaries of zone 2 (to avoid solver complications for the solution of all mono-phase flow equations used in the model), the amount of free air is calculated according to a polynomial (Fig. 3). The polynomial well approximates[3] the theoretical line and it is characterized by a null first derivative at (p - p_{VAPL})/(p_{SAT} - p_{VAPL}) = 0 and at (p - p_{VAPL}) / (p_{SAT} - p_{VAPL}) = 1. Once the free gas fraction, α, is known, the amount of free air is given by $\chi \cdot \alpha$, where χ is the volume content of air at reference conditions.

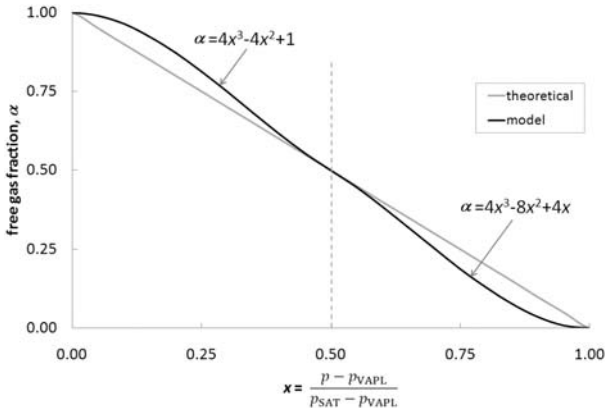

Fig. 3: *Polynomial expression used instead of the Dalton-Henry law*

The calculation of fluid properties is based on a definition of a specific initial state. For convenience, the initial state is described based on a unit volume, V^*, of mixture at temperature T_0 assuming all air released. At these conditions, putting the volumes of the liquid and gas (air) phases at saturation pressure, these are given by:

$$\begin{aligned} V^*_{liq} &= 1-\chi \\ V^*_{gas} &= \chi \end{aligned} \tag{2}$$

For the considered volume the related masses and densities are:

$$\begin{aligned} m_{liq} &= \rho_{L0}(1-\chi) \\ m_{gas} &= \chi\rho_{G0} \\ \rho_{liq} &= \rho_{L0} \\ \rho_{gas} &= \rho_{G0} \end{aligned} \tag{3}$$

At a generic value of $p < p_{SAT}$, the same mass of mixture is characterized by a different amount of released air, according to Fig. 3. Therefore, considering the volumes at $p = p_{SAT}$:

$$\begin{aligned} V^*_{liq} &= 1-\chi \\ V^*_{gas} &= \chi\alpha \\ m_{liq} &= \rho_{L0}(1-\chi)+(1-\alpha)\chi\rho_{G0} \\ m_{gas} &= \chi\alpha\rho_{G0} \end{aligned} \tag{1}$$

The expression for m_{liq} of Eq. 1 includes the mass contribution of the dissolved air into the liquid. From Eq. 1, it is possible to derive the densities related to the two phases:

$$\begin{aligned} \rho_{liq} &= \rho_{L0} + \frac{(1-\alpha)\chi\rho_{G0}}{1-\chi} \\ \rho_{gas} &= \rho_{G0} \end{aligned} \tag{2}$$

Expressions for volumes in Eq. 1 are valid for $p = p_{SAT}$, the pressure that defines the value of ρ_{L0} and ρ_{G0}. Considering the actual pressure for the liquid phase, the volume becomes:

$$V^*_{liq} = \frac{\rho_{L0}}{\rho_L(p,T)}(1-\chi) \tag{3}$$

While for the gas phase, the volume can be calculated assuming a change of temperature form T_0 to T, then a change of pressure from p_0 to p with a polytrophic exponent, γ_G, selected by the user:

$$V^*_{gas} = \frac{\chi\alpha T}{T_0}\left(\frac{p_0}{p}\right)^{\frac{1}{\gamma_G}} \tag{4}$$

By dividing the total mass, given by $m_{liq}+m_{gas}$ of Eq. 1, by the total volume $V^*_{liq}+V^*_{gas}$ given by Eq. 3 and Eq. 4, it is possible to obtain:

$$\rho(p,T) = \frac{(1-\chi)\rho_{L0} + \chi\rho_{G0}}{(1-\chi)e^{\left(\frac{p_{SAT}-p}{K_0(T)}\right)} + \chi\alpha\frac{T}{T_0}\left(\frac{p_{SAT}}{p}\right)^{\frac{1}{\gamma_G}}} \tag{5}$$

Where in Eq. 3 it has been assumed[4]:

$$\rho_L(p,T) = \rho_{L0}\cdot e^{\frac{p-p_{SAT}}{K_0(T)}} \tag{6}$$

From deriving Eq. 5, it is also possible to obtain the analytical expression of the derivative term $\left(\frac{\partial p}{\partial \rho}\right)_T\Big|_{p^*,T^*}$.

2.3 Zone 3: Liquid + Free Air + Vapour

For $p_{VAPL} < p < p_{VAPH}$, fluid is considered as a uniform mixture of liquid, free air and vapour. Similarly to zone 2, the amount of free air is given by Eq. 1. Vapour fraction, Ψ, is null for $p = p_{VAPH}$ and equal to one for $p = p_{VAPL}$. Therefore, the model considers the evaporation of liquid in a range of pressure defined by the user. In this way, the phase change of liquids given by components of different chemical nature (like mineral oils) can be easily simulated. Values for p_{VAPH} and p_{VAPL} can

3 From Fig. 3 it is possible to notice a slight underestimation of the free gas fraction for $x > 0.5$. This is consistent with the real air release process, which is not an instantaneous process as assumed in the model.

4 For $p < p_{SAT}$ it is considered the available values of bulk modulus at saturation pressure dependent on temperature. This values is indicated with $K_0(T)$ in Eq. (9).

be deducted from literature (Tillner et al., 1993 and Washio et al., 2001). In order to guarantee continuity of the equations' first derivative, the model adopts a polynomial expression for the calculation of Ψ with a formulation similar to that used for α (Fig. 3).

The calculation of fluid density in this zone follows passages similar to that described for zone 2, considering that only the mass fraction (1-Ψ) is liquid and with the addition of the vapour phase:

$$V_{vap}^{*} = \frac{\rho_{L0}}{\rho_{V0}} \Psi \frac{T}{T_0} \left(\frac{p_{VAPH}}{p} \right)^{\frac{1}{\gamma_V}}$$

$$\rho_{vap} = \rho_{V0} \frac{T_0}{T} \left(\frac{p}{p_{VAPH}} \right)^{\frac{1}{\gamma_V}} \qquad (7)$$

$$m_{vap} = \rho_{L0} \Psi$$

In Eq. 7, the pressure taken as reference for the polytrophic process is p_{VAPH}, considering that for $p = p_{SAT}$ there is no vapour. Simplifying the description of vapour behaviour, assuming the equation for ideal gas:

$$\rho_{V0} = \frac{p_{VAPH} \cdot m_r}{\tilde{R}_G \cdot T_{G0}} \qquad (8)$$

where, for mineral oil, $m_r \approx 200$ g/mol.

Considering all three phases (liquid, gas, vapour) as in uniform:

$$\rho(p,T) = \frac{(1-\chi)\rho_{L0} + \chi\rho_{G0}}{A+B+C}$$

$$A = (1-\chi)(1-\Psi) e^{\left(\frac{p_{SAT}-p}{K_0(T)} \right)}$$

$$B = \frac{\rho_{L0}(1-\chi)\Psi T}{T_0 \rho_{V0}} \left(\frac{p_{VAPH}}{p} \right)^{\frac{1}{\gamma_V}} \qquad (9)$$

$$C = \frac{\chi \alpha T}{T_0} \left(\frac{p_{SAT}}{p} \right)^{\frac{1}{\gamma_G}}$$

Once again the term $\left(\frac{\partial p}{\partial \rho} \right)_T \Big|_{p^*,T^*}$ comes from the derivative of Eq. 9.

2.4 Zone 4: Free Air + Vapour

In this region, air is assumed to be completely released, and the liquid fully evaporated. The expression for the mixture density (and, consequently, of its derivative) can be derived from Eq. 9 assuming $\alpha = \Psi = 1$.

Figures 4, 5, and 6 show predictions provided by the described fluid model in terms of fluid density and $\partial p/\partial \rho$ for mineral oil HLP32 (the same oil used for tests performed in this work). The Bunsen coefficient, χ, was assumed to be 9 %, a value typical for mineral oil (Ivantysyn and Ivantysynova, 2000). Four different regions of the pressure domain are highlighted. Pressure values higher than p_{SAT} (zone 1) is given by experimental data, according to the measured bulk modulus. Pressure values below p_{SAT} show a significant decrement in density, due to gas cavitation (zone 2), followed by a sudden drop when p_{VAPH} is reached. Below p_{VAPL} (zone 4) the density value is reduced by almost three orders of magnitude, compared to typical liquid values.

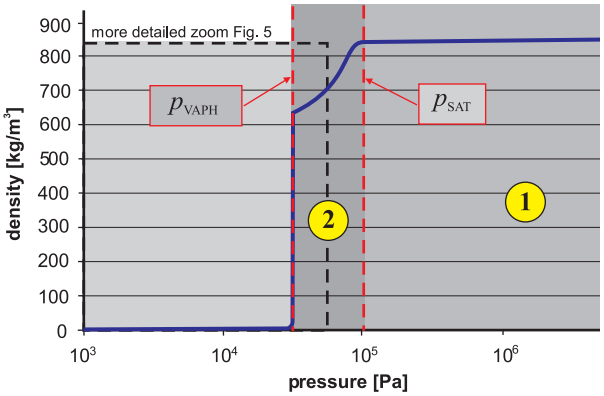

Fig. 4: *Oil density: regions 1 and 2 considered by the numerical model (χ = 9 %; T = 50 °C)*

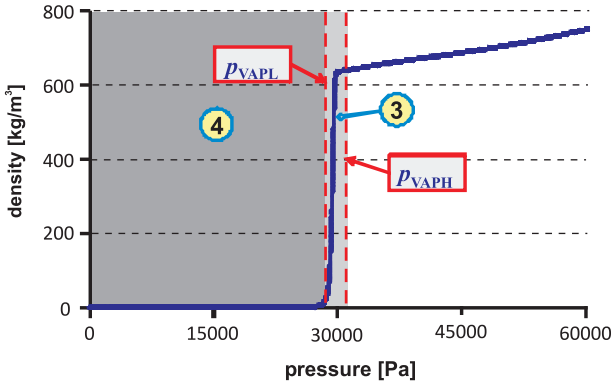

Fig. 5: *Oil density: regions 3 and 4 considered by the numerical model (χ = 9 %; T = 50 °C)*

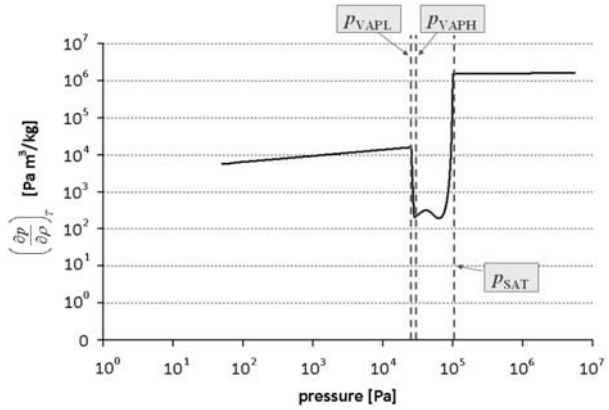

Fig. 6: *Derivative of pressure over fluid density (χ = 9 %; T = 50 °C)*

According to continuum methodology used to describe the fluid, the importance of Fig. 6 lies in the meaning of the partial derivative of pressure with respect to density; this term has a direct influence on the speed of sound for a uniform mixture, being:

$$a = \sqrt{\left(\frac{\partial p}{\partial \rho} \right)_s} \qquad (10)$$

The strong reduction of the partial derivative of

pressure with respect to density is noticeable in Fig. 6[5] when $p < p_{SAT}$ is consistent with what is found in previous researches on cavitation, where a significant reduction of the speed of sound was highlighted in presence of cavitation phenomena (Takahashi et al., 2003; Tillner et al., 1993), as effect of the disturbance of gas bubbles on wave propagation. For $p < p_{VAPL}$ fluid is described by only the gas phase. This explains higher values of speed of sound.

3 The Pump/Motor Simulation Model

The presented model has been implemented within the pressure module of CASPAR. The main structure of the program closely resembles that by Wieczorek and Ivantysynova (2002). Figure 7 illustrates the framework of the model based on a lumped parameter approach. Flow from each displacement chamber to and from both ports through the valve plate is calculated based on opening areas $A_{vpLP,i}$ and $A_{vpHP,i}$. The presented model is also capable of considering special valve plate designs such as pre-compression filter volumes (PCFV); flow into and out of the PCFV depends on $A_{vpPCFV,i}$. The test unit used in this study utilizes this special design feature. In order to realize oscillations in pressure and flow at both ports, constant opening areas A_1 and A_2 along with constant boundary pressures are used; these values are adjusted to achieve desired mean pressures at the ports.

Pressures in each displacement chamber denoted by subscript i, both ports, and the PCFV are determined by solving a set of pressure build up equations based on conservation of mass. Figure 8 illustrates flows entering and exiting a control volume of one displacement chamber.

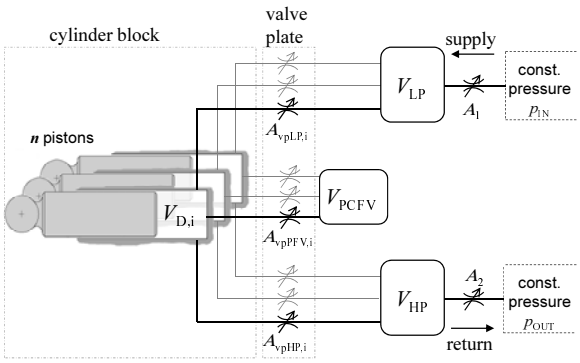

Fig. 7: *Basic model for pump simulation*

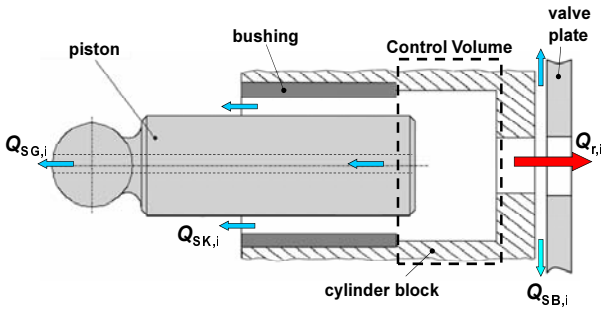

Fig. 8: *Displacement chamber pressure control volume*

The pressure build equation for one displacement chamber considering independent densities for each flow is as follows.

$$\frac{dp_{D,i}}{dt} = \frac{1}{V_{D,i}} \cdot \left(\frac{\partial p_{D,i}}{\partial \rho}\right)_T \cdot \left(\dot{m}_{r,i} + \rho_{SG,i} Q_{SG,i} - \rho_{SK,i} Q_{SK,i} - \rho_{SB,i} Q_{SB,i} - \rho_{D,i} \frac{dV_{D,i}}{dt}\right) \quad (11)$$

Volumetric leakage flows between the valve plate and cylinder block, $Q_{SB,i}$, piston and cylinder bore, $Q_{SK,i}$, and slipper and swash plate $Q_{SG,i}$, are taken into account by the Gap module of CASPAR. The Gap module solves lubricating gap laminar flows on the basis of Reynold's equation, determining the geometry of the self-adjusting gaps (Wieczorek and Ivantysynova, 2002). The volume of the displacement chamber changes throughout one shaft revolution and is taken into account by the term

$$\frac{dV_{D,i}}{dt} = v_{K,i} \cdot A_{K,i} \quad (12)$$

where $v_{K,i}$ and $A_{K,i}$ represent the velocity of the piston and the area of the piston, respectively. The resultant mass flow, $\dot{m}_{r,i}$, is calculated by the orifice equation written for each port separately to capture any cross-flow between high and low pressure ports.

$$\dot{m}_{HP,i} = \rho_{DS} \cdot \alpha_D \cdot A_{vpHP,i} \cdot \frac{p_{HP} - p_{D,i}}{|p_{HP} - p_{D,i}|} \cdot v_{idHP,i} \quad (13)$$

$$\dot{m}_{LP,i} = \rho_{DS} \cdot \alpha_D \cdot A_{vpLP,i} \cdot \frac{p_{D,i} - p_{LP}}{|p_{D,i} - p_{LP}|} \cdot v_{idLP,i} \quad (14)$$

$$\dot{m}_{PCFV,i} = \rho_{DS} \cdot \alpha_D \cdot A_{vpPCFV,i} \cdot \frac{p_{D,i} - p_{PCFV}}{|p_{D,i} - p_{PCFV}|} \cdot v_{idPCFV,i} \quad (15)$$

$$\dot{m}_{r,i} = \dot{m}_{LP,i} + \dot{m}_{HP,i} + \dot{m}_{PCFV,i} \quad (16)$$

Flows entering or exiting the displacement chamber from both ports are dependent on downstream density, ρ_{DS}. For example, flow exiting the displacement chamber into the HP port depends on density of the port, $\rho_{DS} = \rho_{HP}$. In case of back flow from the HP port to the displacement chamber, $\rho_{DS} = \rho_{D,i}$.

Note that, in this form of the orifice equation, it is possible to consider the influence of pressure and temperature on fluid density, and consequently on the ideal (isentropic) speed.

5 $\left(\frac{\partial p}{\partial \rho}\right)_T$ is used in this work as approximation of $\left(\frac{\partial p}{\partial \rho}\right)_s$. This is a good approximation for the liquids (zone 1) where for the entropy: $s = s(p, T) \cong s(T)$.

$$v^2_{\mathrm{id}} = \int_{p_2}^{p_1} \left(dp/\rho \right)_{\mathrm{s}} \tag{17}$$

Figure 9 illustrates the enthalpy vs. entropy representation of compressible flow across an orifice comparing a standard case with a case with sonic (choked) conditions.

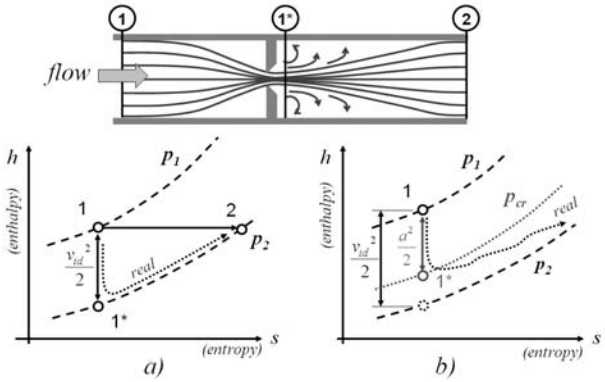

Fig. 9: *Enthalpy vs. entropy representation of compressible flow across an orifice: standard case (a) and presence of sonic (chocked) conditions (b)*

Due to low values of $\left(\partial p/\partial \rho\right)_T$ for mineral oils, highlighted in Fig. 6, sonic conditions can easily occur where one of the two CVs connected by an orifice is characterized by $p < p_{\mathrm{SAT}}$ (usually happens at LP connections for open circuit pumps or motors). To account for these conditions, the model assumes a nozzle's behaviour; the minimum value between the speed of sound given by Eq. 17 and that given by Eq. 10 is taken as the value for ideal velocity when calculating flow across an orifice.

In order to avoid a significant increase of simulation time, compared to a standard lumped parameter model that utilizes a constant (average) value of density for the evaluation of ideal velocity, the proposed model utilizes pre-calculated look up tables. At the beginning of the simulation, the program calculates look up tables of values $\int_0^p \left(dp/\rho \right)_{\mathrm{s}}$, varying p; these values are then used during the simulation to evaluate ideal velocities across each orifice.

Pressure build up equations for the HP and LP port are written based on mass flow entering and exiting the control volume.

$$\frac{dp_{\mathrm{HP}}}{dt} = \frac{1}{V_{\mathrm{HP}}} \cdot \left(\frac{\partial p_{\mathrm{HP}}}{\partial \rho} \right)_{\mathrm{T}} \cdot \left(\sum_{\mathrm{i}=1}^{n_{\mathrm{p}}} \dot{m}_{\mathrm{rHP,i}} - \dot{m}_2 \right) \tag{18}$$

$$\frac{dp_{\mathrm{LP}}}{dt} = \frac{1}{V_{\mathrm{LP}}} \cdot \left(\frac{\partial p_{\mathrm{LP}}}{\partial \rho} \right)_{\mathrm{T}} \cdot \left(\dot{m}_1 - \sum_{\mathrm{i}=1}^{n_{\mathrm{p}}} \dot{m}_{\mathrm{rLP,i}} \right) \tag{19}$$

where $\dot{m}_1$ and $\dot{m}_2$ represent mass flow rates across boundary orifices with openings areas A_1 and A_2, respectively. These mass flow rates are calculated with the same formulation of Eq. (13 to 15 using calculated ideal velocity.

The flow through the pump is simulated solving all the described pressure build up equations and calculating the flow on the basis of the resultant pressures in the defined control volumes. In order to solve the pressure build up equations, the implemented code utilizes a conditionally stable Runge-Kutta method (4th order with step size control, as described in Hoffman (1992)).

A system of equations comprised of pressure build up equations is solved using a 4th order Runge-Kutta variable step solver implemented in the code.

By observing the system, one can highlight how the described fluid model (Section 2) largely affects the calculation of effective flow rate. Contrary to standard lumped parameter models that restrict the influence of pressure and temperature only on ρ and K[6], the effect of fluid compressibility is taken into account in a more thorough way, considering aspects that can play an important role in the simulation of open circuit pumps. More precisely:

- pressure build equations
  Effects of fluid properties are considered separately, regarding terms $\left(\partial p/\partial \rho\right)_{\mathrm{T}}$ and ρ. In this way, calculations of pressure in each CV are more accurate for cases where connected CVs have different pressure values, thus, very different values of density. Figure 10 illustrates the case where the position of one cylinder is open to both ports simultaneously; separately considering terms $\left(\partial p/\partial \rho\right)_{\mathrm{T}}$ and ρ is critical.
- calculation of flow rates
  Equations for compressible flows are used for the evaluation of flow across an orifice regarding unequal values of densities. Ideal velocity is accurately evaluated and flow rate is bounded by sonic (choked) conditions.

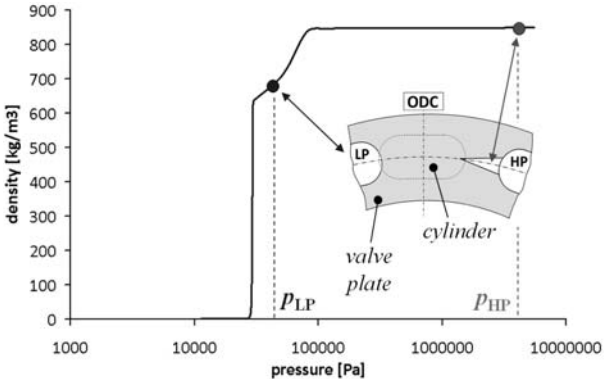

Fig. 10: *Cylinder transition from LP to HP for an open circuit pump. Cylinder's flow (from LP and HP) can be subjected to different values of density*

4 Simulation Results

The proposed model was used to run simulations for an open loop pump at various operating conditions with additional focus on those which may result in insufficient filling. Simulation studies were made using

6 K can be expressed in the pressure build up equations considering the incompressible formulation being: $K = \rho \cdot \left(\frac{\partial p}{\partial \rho} \right)_{\mathrm{T}}$ This form implies the assumption of equal values for all density terms.

a 46 cc open circuit swash plate type axial piston pump. This particular unit was chosen for a simulation study because it was available for experimental measurements as well, as described in the next section. Figure 11 illustrates normalized effective flow rate, Q_{HP}/Q_{ref}, as a function of normalized speed, n/n_{max}. This plot shows the ability of the developed model to predict the drop of effective flow rate at the pump outlet when cavitation occurs at the inlet. Moreover, it shows a comparison with the proposed model considering cavitation with a simpler model that evaluates fluid density and $\left(\partial p/\partial\rho\right)_s$ by simply extending zone 1 (see Fig. 1). This simplification is a common lumped parameter approach used for the simulation of positive displacement machines. The simpler model extrapolates experimental values of density taken at $p > p_{ATM}$ throughout the entire pressure range, thus, incurring errors at $p < p_{ATM}$. Such errors result in inaccurate approximations of effective flow rate at conditions of insufficient filling, high shaft speed and low inlet pressure. Figure 11 shows that a simplified model provides good approximations only for speed ranges of $n < 0.8 \cdot n_{max}$.

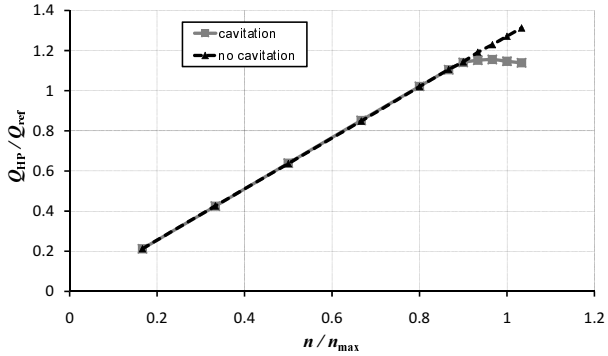

Fig. 11: *Simulated effective flow rate with and without cavitation effects (p_{HP} = 0.25 p_{max}, p_{LP} = 1.2 p_{ATM}, β - 100 %)*

In order to better describe how the proposed model considers fluid cavitation, detailed simulation results of two different conditions of the characteristic shown in Fig. 11 are discussed further: (1) an operating condition where there is an absence of insufficient flow ($n = 0.33 \cdot n_{max}$) and (2) an operating condition resulting in clear cavitation effects ($n = n_{max}$).

Figure 12 illustrates normalized cylinder pressure, p_D, and density of one displacement chamber over one revolution at operating condition $n = 0.33 \cdot n_{max}$; cylinder pressure is higher than the saturation pressure for a large part of the suction stroke (only for a small interval immediately after the IDC, p_D is slightly lower than p_{SAT}). This implies small variation of fluid density, as shown in the same figure.

Figure 13 illustrates normalized mass flow rates entering the displacement chamber during one complete shaft revolution at operating condition $n = 0.33 \cdot n_{max}$. As expected, the PCFV is shown to have a positive effect; backflow from V_{HP} to the cylinder at the beginning of the delivery stroke is significantly limited. The remaining part of flow from the cylinder to HP follows a sinusoidal motion of the piston due to pump kinematics. Similar considerations can be made for flow from V_{LP}; in this case after an initial backflow, the trend follows the motion of the piston.

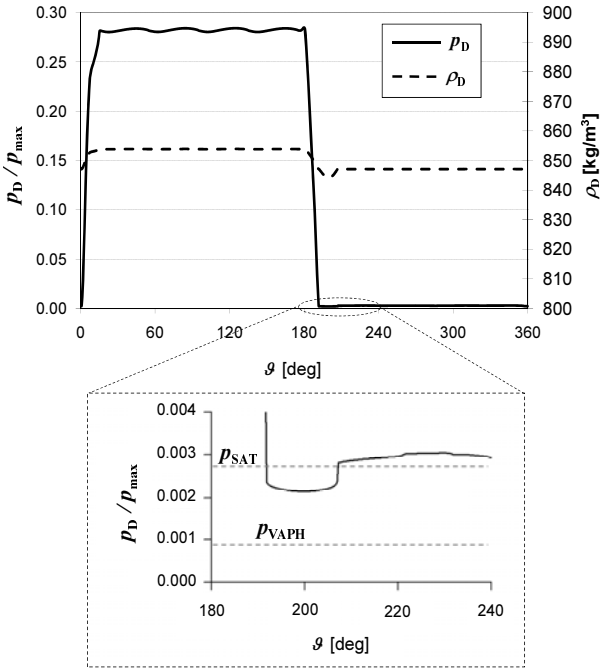

Fig. 12: *Simulated cylinder pressure and density at $n = 0.33 \cdot n_{max}$*

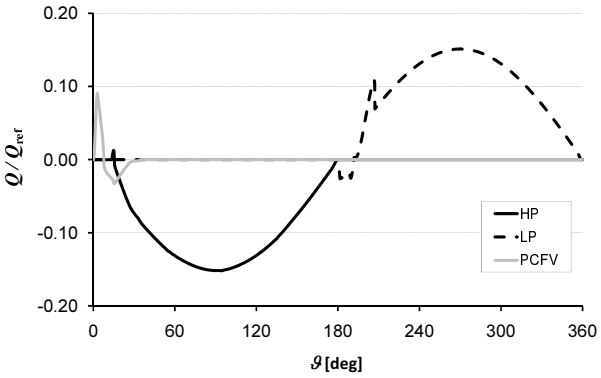

Fig. 13: *Simulated cylinder mass flow rates with LP, HP, and PCFV control volumes at $n = 0.33 \cdot n_{max}$ ($Q > 0$ signifies flow entering the cylinder)*

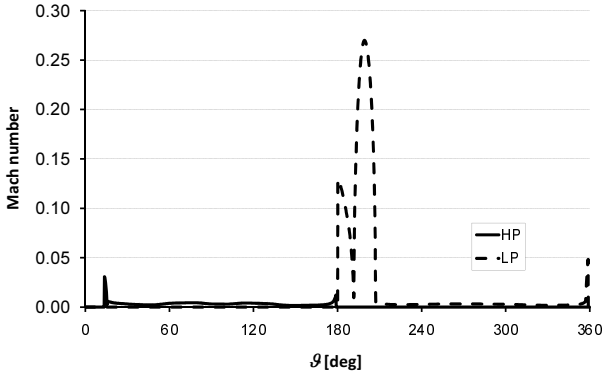

Fig. 14: *Simulated Mach number for HP and LP cylinder flows of Fig. 12 at $n = 0.33 \cdot n_{max}$*

Figure 14 reports the ratio between instantaneous fluid velocity and sound speed related to HP and LP flows at operating condition $n = 0.33 \cdot n_{max}$. It is important to notice how this ratio is always lower than 0.3;

this is later compared with Mach numbers at $n = n_{max}$.

Figures 15, 16 and 17 report the same quantities of Fig. 12, 13 and 14, but for the operating condition at $n = n_{max}$. Figure 15 illustrates lower values for cylinder pressure, pD, during the suction stroke with respect to that of Fig. 12; this is due to higher piston speeds (that derives from the higher shaft speed). Cylinder pressure drops lower than p_{SAT} for the entire suction stroke, causing a fluid density significantly lower than that corresponding to the delivery stroke. Therefore, volumetric flow rate is attenuated due to high requests of flow and an increase of specific volume.

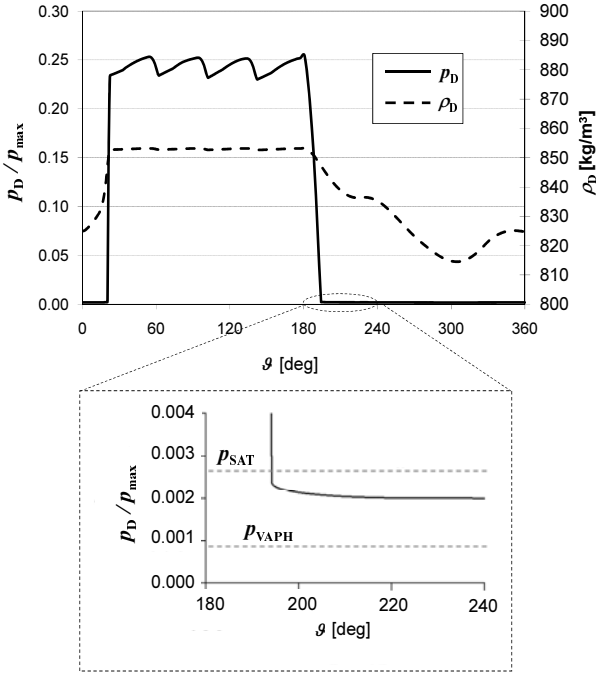

Fig. 15: *Simulated cylinder pressure and density at $n = n_{max}$*

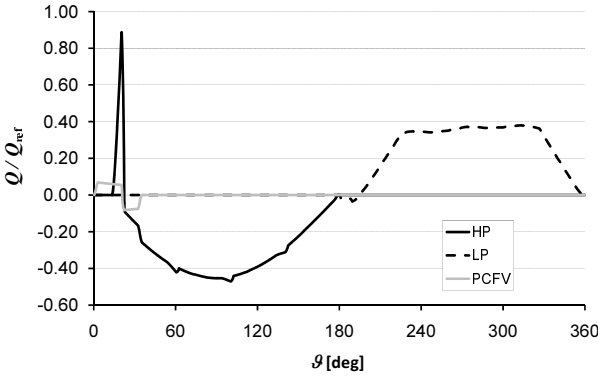

Fig. 16: *Simulated cylinder mass flow rates with LP, HP, and PCFV control volumes at $n = n_{max}$*

Figure 16 illustrates normalized mass flow rates; at the high speed condition $n = n_{max}$, the PCFV is not sufficient to avoid backflows from V_{HP} at the beginning of the delivery stroke. It is important to note the different trend of flow rate $Q_{LP,i}$, that characterizes the suction stroke with respect to that shown in Fig. 13[7]. This can be explained by the compressible fluid approach used by the proposed model, which limits the drop of p_D by accurately calculating an increased specific volume of the fluid during the suction stroke.

Figure 17 displays normalized Mach number of HP and LP flows at the high speed operating condition $n = n_{max}$; for a large part of the suction stroke the predicted Mach number related to $Q_{LP,i}$. is greater than 0.3. This value is typically considered as the limit of applicability of incompressible models for the description of flow (Shaughnessy et al, 2005). For all conditions considered in this work it has been found that when the average Mach number related to Q_{LP} is greater than 0.3, the predictions given by the simple model which neglects the effects of cavitation are different than results obtained using the presented model. Therefore, as shown in Fig. 11, the point where both curves separate can be interpreted as the upper limit of application of standard lumped parameter models used for the simulation of open circuit pumps which neglect effects due to cavitation.

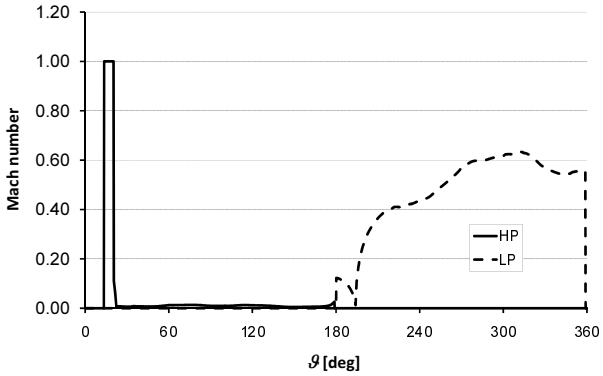

Fig. 17: *Simulated Mach number for HP and LP cylinder flows of Fig. 15 at $n = n_{max}$*

Regarding flow Q_{HP}, Fig. 17 illustrates how the corresponding Mach number is very low for the delivery stroke, with the exception of an initial backflow necessary to pressurise the displacement chamber in proximity of ODC, where Mach = 1; at this condition, flow is assumed to be sonic.

5 Experimental Verification of the Model

The proposed model has been benchmarked to evaluate its validity and potentials through experiments performed at the MAHA Fluid Power Laboratory using a swash plate type axial piston pump for open circuit applications. The objective of the experiments was to measure effective flow rate under conditions of insufficient suction flow due to cavitation. Measurements were made on the same 46 cc open circuit swash plate type axial piston pump as used for the simulation study. To achieve conditions of insufficient filling, the pump was tested at higher speeds than the manufacturer recommends; i.e. n_{max} chosen for this experiment was higher than n_{max} recommended by the manufacturer.

7 Using the prediction of the simplified model used to obtain results of Fig. 11, that neglects both gas and vapour cavitation, at the highest speed p_D drops to negative (not physical) values during the suction stroke. With the proposed model, however, the trend of mass flow rate entering the cylinder keeps the typical sinusoidal trend of Fig. 13 also at high speeds.

An ISO schematic of the test rig is shown in Fig. 18. By means of pressure compensated pumps, the hydraulic power supply connected to the system maintains a constant value of pressure (≈ 10 bar) upstream OR1 for all the conditions considered in this work. A variable orifice is placed at the inlet of the pump in order to achieve low inlet pressure conditions. A second variable orifice is placed at the outlet of the pump to set the desired load on the unit. A picture of the test rig setup is shown in Fig. 19. Table 1 displays more detailed information of sensors and equipment used on the test rig.

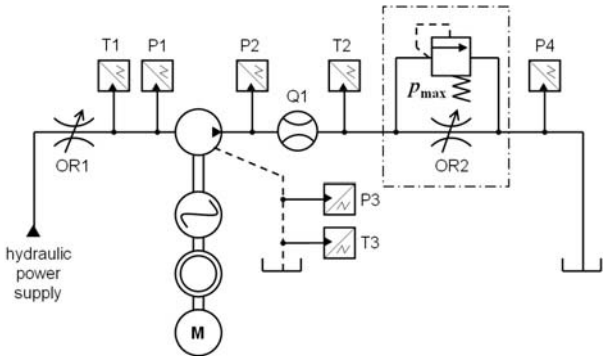

Fig. 18: *ISO schematic of the test circuit*

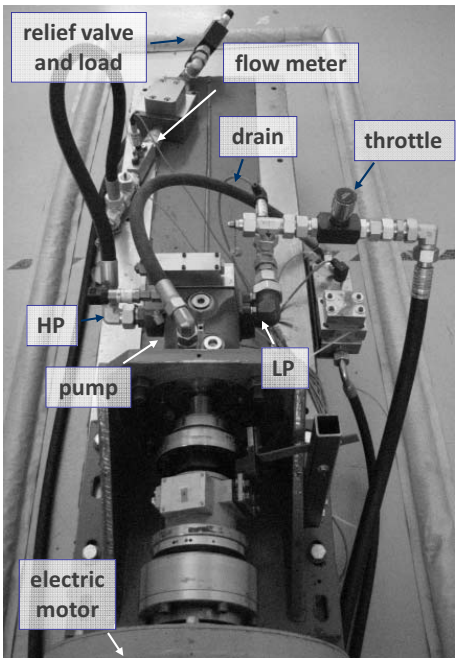

Fig. 19: *Picture of the test rig*

In order to emphasize conditions of insufficient inlet flow due to cavitation, two types of tests were carried out. All test conditions are normalized according to max pressure and speed for confidentiality reasons.

Test type 1 (t1): constant HP, LP pressure, varying shaft speed:

In these tests, the effective flow rate of the pump was measured for different shaft speeds. At each shaft speed, orifices OR1 and OR2 were manually adjusted in order to obtain desired values of p_{HP} and p_{LP}, according to the test plan reported in Table 2.

Test type 2 (t2): constant shaft speed and HP pressure, varying LP pressure:

Measurements of effective flow rates were carried out varying suction pressure by manually adjusting the OR1 opening area. As reported in Table 2, different values of shaft speed and delivery pressure were taken into account for this kind of test.

Table 1: Sensors and equipment used

Feature	Type	Main features
T1, T2, T3	resistive	Omega K-type thermocouple, range 0 - 120 °C; 1 % FS accuracy
P1, P3, P4	strain gage	WIKA® , Scale: 0 - 25 bar, 0.25 % FS accuracy
P2	strain gage	WIKA®, Scale 0 - 600 bar, 0.25 FS accuracy
Q1	flow meter	Flo-tech turbine flow meter, range 0 - 150 L/min; 1 % FS accuracy
T	speed, torque meter	HBM® MC60, Scale: 0; 500 Nm, 5000 r/min-1 Limit Velocity, 0.05 Accuracy Class
OR2	needle valve	Sun hydraulics®, maximum flow 400 L/min
OR1	needle valve	Anchor Fluid Power® maximum flow 400 L/min
M	electric motor	SSB, 500 Nm; max speed: 3000 r/min

Table 2: Measurement parameter setting

Test type 1			
Test no.	p_{HP}	p_{LP}	n
t1.1	$0.25 \cdot p_{max}$	$2 \cdot p_{ATM}$	$(0.33 - 1) \cdot n_{max}$
t1.2	$0.25 \cdot p_{max}$	$1.5 \cdot p_{ATM}$	$(0.33 - 1) \cdot n_{max}$
t1.3	$0.25 \cdot p_{max}$	$1.2 \cdot p_{ATM}$	$(0.33 - 1) \cdot n_{max}$
t1.4	$0.5 \cdot p_{max}$	$2 \cdot p_{ATM}$	$(0.33 - 1) \cdot n_{max}$
t1.5	$0.5 \cdot p_{max}$	$1.5 \cdot p_{ATM}$	$(0.33 - 1) \cdot n_{max}$
t1.6	$0.5 \cdot p_{max}$	$1.2 \cdot p_{ATM}$	$(0.33 - 1) \cdot n_{max}$
Test type 2			
Test no.	p_{HP}	p_{LP}	n
t2.1	$0.25 \cdot p_{max}$	$< 1.1 \cdot p_{ATM}$	$0.33 \cdot n_{max}$
t2.2	$0.5 \cdot p_{max}$	$< 1.1 \cdot p_{ATM}$	$0.33 \cdot n_{max}$
t2.3	$0.25 \cdot p_{max}$	$< 1.1 \cdot p_{ATM}$	$0.66 \cdot n_{max}$
t2.4	$0.5 \cdot p_{max}$	$< 1.1 \cdot p_{ATM}$	$0.66 \cdot n_{max}$
t2.5	$0.25 \cdot p_{max}$	$< 1.1 \cdot p_{ATM}$	n_{max}
t2.6	$0.5 \cdot p_{max}$	$< 1.1 \cdot p_{ATM}$	n_{max}

All 12 tests were performed using a Keithly DAS 1802HC data acquisition system and the software Test Point.

In all tests, T_{LP} (given by sensor T1) was set to ≈ 45 °C, and the measured increment of temperature at

delivery (T2) and at the drain line (T3) was always less than 5 °C.

All experiments performed were also simulated using the proposed model. The properties of fluid used for the test (HLP32, a ISO VG 32 mineral base oil) have been reproduced with the model described in Section 2, assuming the parameters of Table 3.

Due to length constraints of this paper, only the most significant comparisons between simulated and experimental results are described. In particular, for both types of tests (t1 and t2), cases where effects of insufficient suction flow are evident are shown for the verification of the proposed model's predictions. For example, for test t1.1 no relevant flow rate reductions due to cavitation were observed, while for test t1.3 a drop of Q_{HP} is evident at the highest speed, as shown in Fig. 20.

Table 3: Fluid model parameters

Parameter	value		Parameter	value
p_{SAT}	101300 Pa		χ	0.09
p_{VAPH}	30000 Pa		γ_G	1.2
p_{VAPL}	25000 Pa		γ_V	1.2
			ρ_{G0}	1.2 kg/m^3

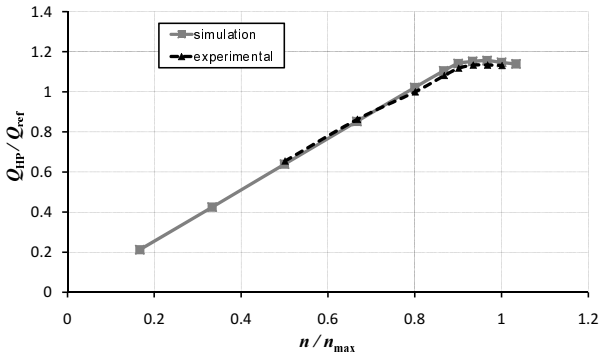

Fig. 20: *Comparison between experimental results and simulation data for case t1.3*

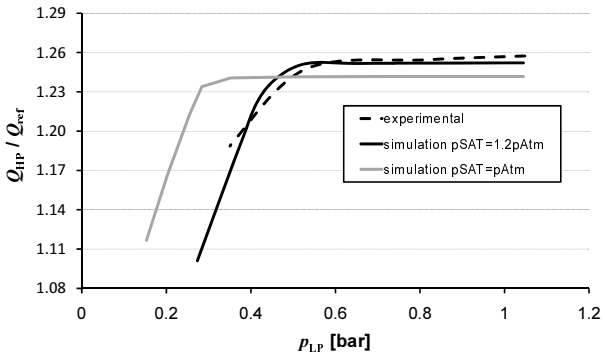

Fig. 21: *Comparison between experimental results and simulation data for case t2.6 of Table 2*

Figure 20 shows normalized effective pump flow, Q_{HP}, as a function of normalized pump speed. The dashed line shows the measured value from experiment and the solid line shows simulation results using the proposed model. The proposed model assumed 9 % air content at $p_{SAT} = p_{ATM}$. All comparisons between measured and simulated data for tests t1 resulted in a good agreement.

Figure 21 illustrates the case t2.6 of Table 2. Experimental results are compared with two simulated results. The difference between the two simulations is the setting for p_{SAT}, which is $1.2 \cdot p_{ATM}$ and $1.0 \cdot p_{ATM}$ in this comparison. The simulation using $p_{SAT} = 1.0 \cdot p_{ATM}$ provided a reasonable agreement within uncertainties of the sensors; however, it turned out that a better matching with experimental results can be found with a slightly increased value of p_{SAT}. Note that fine tuning a value of p_{SAT} was possible with tests t2 due to the fact that results are represented on a more detailed scale; differences between various trends are emphasized. Furthermore, comparing measured data from tests t1 with simulated results using $p_{SAT} = 1.2 \cdot p_{ATM}$ also showed improvements.

For all conditions of Table 2, the minimum values of pressure p_D were found to be significantly greater than p_{VAPH}. This is a confirmation of deductions also reported in literature, such as IMAGINE SA (2007) and Casoli et al. (2006), where it is highlighted how vapour cavitation is typically a local phenomena of zones characterized by high fluid velocity and low pressure; for fluid power components, even at extreme conditions, entire volumes have difficultly achieving $p < p_{VAPH}$.

6 Conclusions

In this paper, a lumped parameter model for the prediction of effective flow rate considering air release and vapour cavitation of axial piston machines is presented. Such an approach is essential for modelling open circuit pumps at conditions of possible insufficient filling. The proposed model is able to simulate conditions of insufficient flow at the delivery port due to fluid cavitation. The model uniquely shows the ability to predict effective flow rate throughout a wide operating range, thus revealing limiting conditions of the machine. In particular, the model solves equations for compressible flow for all possible operating conditions of the machine, assuming the fluid as a continuum, where gaseous phases can be present as effect of both gas and vapour cavitation. The amount of air released and oil vapour is calculated through equilibrium equations, thus establishing the amount of different phases (liquid, gas) of the continuum as a function only of pressure and temperature. Basic equations for monophase, compressible flows used in the model consider the possible limitations of flow rate due to sonic conditions. It is shown that relevant compressibility effects, and in some cases choking conditions, can occur in presence of cavitation. Moreover, the evaluation of sound speed also permits criticism in the interpretation of simulation results by identifying regions where standard, incompressible approaches can provide approximately the same estimation of the presented model.

Two different types of tests were performed on an open circuit pump with the aim of describing the onset of insufficient suction flow due to cavitation. Simulations of tested conditions show a high level of accurate prediction using the developed tool; the effective flow rate is well estimated by the code in presence of insuf-

ficient suction flow due to cavitating conditions.

A proper implementation of the model requires a simulation time comparable to other lumped parameter models used to simulate this kind of machine. Although the model does not predict detailed features of cavitation phenomena (i.e. features of bubble formation and collapse), detailed analysis of simulation results permits a better understanding of the phenomena involved in the operation of the pump relating to incipient cavitation at the LP port. Furthermore, the parameters used for the description of fluid properties (i.e. saturation and vapour pressures, volumetric air content, etc.) permits a better reproduction of experimental conditions, in agreement to the typical philosophy of lumped parameter approaches.

Nomenclature

a	Sound speed	[m/s]
A	Orifice opening area	[m^2]
h	Enthalpy	[Pa]
K	Bulk modulus	[kg]
m	Mass	[kg]
$\dot{m}$	Mass flow rate	[kg/s]
m_r	Oil vapour molecular mass	[g/mol]
n	Shaft speed	[rpm]
n_p	Number of pistons	[-]
p	Pressure	[Pa]
Q	Volumetric flow rate	[m^3/s]
R_G	Gas constant	[J/kmol]
s	Entropy	[J/K]
t	Time	[s]
T	Temperature	[°C]
v	Velocity	[m/s]
V	Volume	[m^3]
V^*	Dimensionless volume	[-]
α	Free gas fraction	[-]
χ	Bunsen Coefficient (air volume content at T_0, p_{SAT})	[-]
ρ	Fluid density	[kg/m^3]
ϕ	Angle	[deg]
ψ	Vapour fraction	[-]

Subscripts

0	Reference conditions
D	Displacement chamber
DS	Downstream
gas	Gas phase
G	Gas properties
i	Index of piston
id	Ideal
k	Piston
liq	Liquid phase
L	Liquid properties
max	Maximum value
r	Resultant
ref	Reference value
s	Constant entropy
SAT	Saturation
T	Constant temperature
V	Vapour properties
vap	Vapour phase
VAPH	Higher saturated vapour
VAPL	Lower saturated vapour

Abbreviations

ATM	Atmospheric
CV	Control Volume
HP	High Pressure
IDC	Inner Dead Centre
LP	Low Pressure
ODC	Outer Dead Centre
PCFV	Pre Compression Filter Volume
vp	Valve Plate

References

Casoli, P., **Vacca, A.**, **Franzoni G.** and **Berta, G. L.** 2006. Modelling of fluid properties in hydraulic positive displacement machines. *Elsevier - Simulation Modelling Practice and Theory*, Vol. 14, pp. 1059–1072.

Delannoy, Y. and **Kueny, J. L.** 1990. Two Phase Flow Approach in Unsteady Cavitation Modeling. *Cavitation and Multiphase Flow Forum, ASME FED*, Vol. 98, pp. 153-158.

Edge, K. A. and **Darling, J.** 1989. The Pumping Dynamics of Swash Plate Piston Pumps. *Journal of Dynamic Systems, Measurement and Control, Trans. of ASME*, Vol. 11, pp. 307-311.

Hoffman, J. D., **1992,** *Numerical methods for engineers and scientists,* Mc Graw Hill.

Hyman, J. M. 1984. Numerical Methods for Tracking Interfaces. *Los Alamos Natl. Lab. Rep. LA-9917-MS*, pp.1-20.

Imagine, S. A. 2007. HYD Advanced Fluid Properties. *Technical Bulletin n° 117*, Rev 7, May 2007.

Ivantysyn, J. and **Ivantysynova, M.** 2000. Hydrostatic Pumps and Motors, Principles, Designs, Performance, Modelling, Analysis, Control and Testing. New Delhi. *Academia Books International*.

Ivantysynova, M., **Grabbel, J.** and **Ossyra, J. C.** 2002. Prediction of swash plate moment using the simulation tool CASPAR. *ASME Int. Mech. Eng. Congress*, Nov. 17-22, 2002, New Orleans, USA.

Kim, S. D., **Cho, H. S.** and**, Lee, C. O.** 1987. A Parameter Sensitivity Analysis for the Dynamic Model of a Variable Displacement Axial Piston Pump. *IMechE Proc, Instn Mech Engrs*, Vol. 201, No. C4.

Klop, R. and **Ivantysynova, M.** 2008. Investigation of Noise Source Reduction Strategies in Hydrostatic Transmissions. *Proc. of the 5th FPNI PhD Symposium*, Cracow, Poland, pp. 63 - 76.

Lamb, W. S. 1987. *Cavitation and aeration in hydraulic systems*. Bedfordshire, UK. BHRGroup. 114.

Manring, N. D. 2000. The Discharge Flow Ripple of an Axial-Piston Swash-Plate Type Hydrostatic Pump. *Journal of Dynamic Systems, Measurement, and Control*, Vol. 122 pp. 263-268.

Palmberg, J. O. 1989. Modelling of flow ripple from fluid power piston pumps. *In 2nd Bath Int. Fluid Power Workshop*, Univ. of Bath, UK, Sept 1989.

Schmidt, D. P. and **Corradini, M. L.** 1997. Analytic Prediction of the Exit Flow of Cavitating Orifices. *Atomization and Sprays*, Vol. 7 pp. 603-616.

Schmidt, D. P., **Rutland, C. J.** and **Corradini, M. L.** 1999. A fully compressibile, two-dimensional model of Small, High-Speed, Cavitating Nozzles. *Atomization and Sprays*, Vol. 9. pp. 225-276.

Schoenau, G. J., **Burton, R. T.** and **Kavanagh, G. P.** 1990. Dynamic Analysis of a Variable Displacement Pump. *Journal of Dynamic System, Measurement, and Control*. Vol. 112, pp.122-132.

Seeniraj, G. and **Ivantysynova, M.** 2008. Noise Reduction in Axial Piston Machines Based on Multi-Objective Optimization. *Proc. of the 5th FPNI PhD Symposium*, Cracow, Poland, pp. 111 - 123.

Shaughnessy, E. J., **Katz, I. M.** and **Schaffer, J. P.** 2005. *Introduction to Fluid Mechanics*. Oxford University Press, New York, USA.

Singhal, A. K., **Athavale, M. M.**, **Li, H.** and **Jiang, Y.** 2002. Mathematical Basis and Validation of the Full Cavitation Model. *Journal of Fluid Engineering*, Vol. 124 pp. 617-624.

Takahashi, S., **Washio, S.**, **Uemura, T.** and **Okazaki, A.** 2003. Experimental Study on Cavitation Starting at and Flow Characteristics Close to the Point of Separation. *5th Int. Symposium on Cavitation*, Osaka, Japan November 1-4, 2003.

Tillner, W., **Fritsch, H.**, **Kruft, R.**, **Lehman, W.** and **Masendorf, D. G.** 1993. *The avoidance of cavitation damage*. MEP, London.

Washio, S., **Takahashi, S.**, **Uda, Y.** and **Sunahara, T.** 2001. Study on cavitation inception in hydraulic oil flow through a long two-dimensional constriction. *IMechE - Proc Instn Mech Engrs*. Vol. 215 Part J, pp. 373-386.

Wieczorek, U. and **Ivantysynova, M.** 2000. CASPAR - A Computer Aided Design Tool for Axial Piston Machines. *Proc. Bath Workshop on Power transmission and Motion Control PTMC 2000*, Bath, UK, pp. 113 - 126.

Wieczorek, U. and **Ivantysynova, M.** 2002. Computer Aided Optimization of Bearing and Sealing Gaps in Hydrostatic Machines - The Simulation Tool CASPAR. *International Journal of Fluid Power*, Vol. 3, No.1, pp. 7-20.

Andrea Vacca
Born on June 2nd 1974, currently Andrea Vacca is Assistant Professor in Mechanical Enginnering at the University of Parma (Italy). At the same University, in 1999, he received his Master's degree in Mechanical Engineering. In 2005 he became Ph. Doctor, at University of Florence, with a thesis in the field of Heat Transfer and Gas Turbine Blade Cooling Technology. His main research interests are the analysis and simulation of fluid power systems and components, such as valves, gear and piston pumps.

Richard Klop
Born on February 18th 1983 in Kalamazoo Michigan (USA). He received his B.S. Degree from Michigan State University, USA, with high honors in Mechanical Engineering in 2005. He received his MSE Degree at Purdue University, USA, in Agricultural and Biological Engineering in 2007. He is a Doctoral student at Purdue University in the area of acoustics and fluid power. His main research interest is noise control concepts for hydrostatic transmissions.

Monika Ivantysynova
Born on December 11th 1955 in Polenz (Germany). She received her MSc. Degree in Mechanical Engineering and her PhD. Degree in Fluid Power from the Slovak Technical University of Bratislava, Czechoslovakia. After 7 years in fluid power industry, she returned to university. In April 1996 she received a Professorship in fluid power & control at the University of Duisburg (Germany). From 1999 until August 2004 she was Professor of Mechatronic Systems at the Technical University of Hamburg-Harburg. Since August 2004 she is Professor in Mechanical Engineering and Agricultural and Biological Engineering at Purdue University, USA. She was approved as Maha named Professor in Fluid Power Systems and director of the Maha Fluid Power Research Center at Purdue University in November 2004. Her main research areas are energy saving actuator technology and model based optimization of displacement machines as well as modeling, simulation and testing of fluid power systems. Besides the book "Hydrostatic Pumps and Motors" published in German and English, she has published more than 90 papers in technical journals and at international conferences.